All-Pass NGD FIR Original Study for Sensor Failure Detection Application

Blaise Ravelo, Mathieu Guerin, Wenceslas Rahajandraibe, Lala Rajaoarisoa

All-Pass NGD FIR Original Study for Sensor Failure Detection Application

Blaise Ravelo, *Member*, *IEEE*, Mathieu Guerin, *Member*, *IEEE*, Wenceslas Rahajandraibe, *Member*, *IEEE*, and Lala Rajaoarisoa, *Member*, *IEEE*

***Abstract*—This paper deals with original design, implementation, test, and potential application of finite impulse response (FIR) with uncommon all-pass negative group delay (AP-NGD) circuit. The counterintuitive AP-NGD numerical circuit theory is established. Design method of first order AP-NGD circuit is introduced with respect to the specified time-advance. The first order difference equation was synthesized, designed, and implemented in STM32® Microcontroller Unit, and experimented to validate the AP-NGD characteristics. The AP-NGD FIR prototype was tested in the time-domain with Gaussian and arbitrary waveform sensored signals. Calculated and experimented results in very good agreement with the most significant time-advance -10 s ever experimented before are obtained. The potential industrial application of the NGD predictor for sensor fault diagnosis in real-time is described.**

***Index Terms*—Numerical circuit design, Negative group delay (NGD) function, Finite Impulse Response (FIR), Time-domain test, All-pass NGD (AP-NGD), NGD numerical circuit, NGD predictor, sensor fault diagnosis.**

NOMENCLATURE

t	Time variable
t_{max}	Maximal time variable
$f=\omega/(2\pi)$	Frequency variable
$f_{max}=\omega_{max}/(2\pi)$	Maximal frequency variable
f_l	Cut-off frequency
$s=j\omega=2j\pi f$	Laplace variable
v_{in}, v_{out}	Input and output voltages
k, n	Positive integer
k_{max}	Maximal positive integer
N	Transfer function
GD	Group delay
t_0	Group delay at $f\approx 0$
f_0	Specific frequency associated to t_0
$f_s = 1/\Delta t = 1/T_s$	Sampling frequency
a_0, a_1	Real coefficients of AP-NGD FIR
A_{in}, A_{out}	Input and output signal amplitude
g	Transient gain between v_{out} and v_{in}
$r(v_{in},v_{out})$	Input and output relative cross-correlation
$\hat{v}_{\psi}$	Average value of (input or output) voltage samples $v_{\psi}(k)$
v_T	Voltage threshold
t_{in}, t_{out}	Input and output voltage instant time where $v_{in}(t_{in}) = v_{out}(t_{out}) = v_T$
$\Delta t = t_{out} - t_{in}$	Transient time-advance
V_{dd}	Voltage supply
$V_{\max}$	Maximal amplitude of input signal
τ	Instant time where $V_{\max} = v_{in}(\tau)$
f_a	Gaussian input signal bandwidth
a_{dB}	Gaussian spectrum attenuation at f_a
f_b	Sinc input signal inverse of period
v_{Calc}, $v_{Meas.}$	Calculated and measured voltages
x, y	Input and output signals
x_n	Reference level of test signals x, y
x_{lim}	Maximal input signal
t_1, t_2, t_3, t_4	Specific instant time of test signals x, y

I. INTRODUCTION

THE FAULT diagnosis of sensors and actuators is the key element to guarantee the modern industrial system performances [1-8]. Different techniques as synchronous sampling and impulse detection [1], observer-based adaptive decentralized fault-tolerant control [2], signal enhancement method [3], simultaneous isolation of sensor and actuator faults [4], adaptive online fault diagnosis of manufacturing systems based on discrete event system specification (DEVS) formalism [5], high accuracy insulation fault diagnosis method based on power maximum likelihood estimation [6] and sensor fault diagnosis in inland navigation networks based on a grey-box model [7-8] were recently proposed. The sensor and actuator diagnosis technique performances depend on measurement and topological information data robustness [9-10]. With the technological progress, the sensor and actuator industrial systems are expected to operate remotely [11-15]. The real-time anomaly detection techniques which, depending on time-delay

Manuscript received xxx xx, 2022; revised xxx xx, 2022; accepted xxx xx, 2022. Date of publication xxx xx, 2022. (Corresponding author: Dr. Mathieu Guerin)

Blaise Ravelo is with the Nanjing University of Information Science & Technology (NUIST), Nanjing 210044, Jiangsu, China (E-mail: blaise.ravelo@yahoo.fr).

Mathieu Guerin, and Wenceslas Rahajandraibe are with the Aix-Marseille University, CNRS, University of Toulon, IM2NP UMR7334, Marseille, France (E-mail: {mathieu.guerin, wenceslas.rahajandraibe}@im2np.fr).

Lala Rajaoarisoa is with IMT Nord Europe, University of Lille, Centre for Digital Systems, F-59000 Lille, France (e-mail: lala.rajaoarisoa@imt-nord-europe.fr).

effect, are needed for the fault diagnosis of such remote operating network systems [13-18]. Different methods allowing to consider the time-delay effect as communication delay [14], system performance optimization [17], asymmetry aspects [18], and estimation [19] were investigated. Delay compensation techniques [20-21] notably for networked control systems in controller area networks were proposed. In addition, different fault system detection and prediction techniques were developed to face up the delay effects [22-25]. One of the most efficient approaches to analyze signal delay in both frequency and time domain can be performed by the group delay (GD) analysis [26]. It is emphasized that certain electronic analog circuits are susceptible to operate with time-advance effect based on the use of uncommon negative GD (NGD) electronic function [24-25,27-35]. It is worth to note that the fascinating NGD time-advance does not contradict the causality [29-30].

Because of its counterintuitive effect, the NGD electronic function is still an uncommon knowledge for non-specialist industrial sensor and actuator design engineers. For the better understanding, the NGD circuit theory analogue to the filter was initiated [27]. The canonical transfer function (TF) of low-pass (LP) NGD analog circuit topology was fundamentally identified and proposed [27-32]. It was theoretically and experimentally demonstrated the possibility to propagate output of smoothed enough input signal in time-advance by using analog circuit [27-32]. Moreover, the time-advance absolute value is limited lower than 1 second with analog circuits [27-32]. So far, most of NGD circuit design and theory available in the literature are typically with LP behaviors which is limited by their NGD cut-off frequency [27-32]. To overcome such a technical limit, innovative design of numerical LP-NGD circuits were proposed in few studies [33-35]. But compared to the research work available in the literature about NGD analog circuit designs, many efforts need to be paid on the NGD numerical circuit. Many curious questions were wondered about the implementability and testability of typical all-pass (AP) NGD finite impulse response (FIR) numerical circuit.

In the present paper, an original research work, never being done before, is introduced about the designability, implementability and testability of typical AP-NGD FIR numerical circuit with time advance absolute value record more than 1 second. The paper is organized in four sections as follows:

- Section II develops the original theory of AP-NGD FIR numerical circuit. The AP-NGD analysis from analog TF to the difference equation is introduced. The design equations enabling to determine the AP-NGD FIR coefficients will be established.
- Section III focuses on the validations of the original AP-NGD FIR with proof-of-concept (POC) and prototype implemented on STM32® microcontroller unit (MCU). The AP-NGD FIR design method will be discussed based on calculated and experimented results with different test signals.
- The real-time fault diagnosis remains a challenging problem for the industrial sensor design engineers [1-8]. To tackle this technical problem, Section IV discusses on potential application of AP-NGD FIR for sensor fault real-time diagnosis. An innovative industrial application of AP-NGD FIR circuit is developed on the real-time failure pre-detection of sensor and actuator systems.
- Then, Section V presents the final conclusion.

II. Theory and Design Method of Original AP-NGD FIR Circuit

The present section is dedicated to the theory of original AP-NGD FIR. The methodology to develop the numerical circuit theory is also described.

A. Definition of AP-NGD Analog TF

The AP-NGD analog TF characterization is elaborated in this subsection. The main particularity of NGD analysis is the simultaneous approach in both the time and frequency domain.

1) Expected Specifications of AP-NGD Test Signal

Like all electronic functions, the innovative AP-NGD circuit must operate under specific requirements of input signals. The *t*-time dependent input signal of AP-NGD circuit can be represented by voltage $v_{in}(t)$. As illustrated by Fig. 1(a), this input voltage $0 \le v_{\min} \le v_{in}(t) \le v_{\max}$ is delimited by minimum v_{min} and maximum v_{max}. In addition, we assume that the test signal is specified by its time duration t_{max} or $v_{in}(t \ge t_{\max}) \approx 0$.

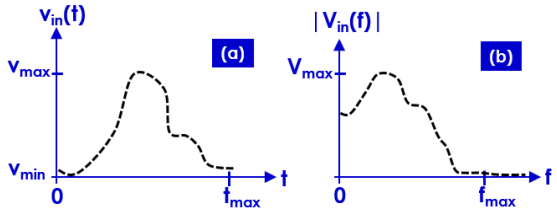

Fig. 1. Typical representation of (a) chronogram and (b) spectrum of AP-NGD input signal.

The input signal frequency spectrum is denoted by $V_{in}(s)$ by taking the Laplace variable $s=j\omega$, with angular frequency variable $\omega=2\pi f$. The magnitude of input signal spectrum $|V_{in}(f)| \le V_{\max}$ can be represented by Fig. 1(b). This spectrum is characterized by the maximum magnitude V_{max} and frequency f_{max} with $|V_{in}(f \ge f_{\max})| \approx 0$.

2) Recall on LP-NGD Specifications

The present NGD theory is based on the voltage TF $N(s)=V_{out}(s)/V_{in}(s)$ associated to V_{in} and output voltage V_{out}. The GD associated to TF N is defined by:

$$GD(\omega) = -\partial \arg[N(j\omega)] / \partial\omega . \quad (1)$$

We recall that the $GD_{LP\text{-}NGD}$ characteristic LP-NGD ideal diagram with NGD value $GD_{LP-NGD}(\omega \approx 0) = t_0 < 0$. Cut-off frequency ω_l is verifying $GD_{LP-NGD}(\omega < \omega_l) < 0$ and $GD_{LP-NGD}(\omega \ge \omega_l) \ge 0$ represented by Fig. 2 [27-33].

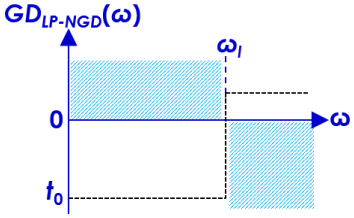

Fig. 2. LP-NGD GD ideal diagram [27-33].

The dashed parts of the graph are the forbidden zone. We have the case of innovative AP-NGD function if the cut-off frequency becomes infinity $\omega_l=+\infty$. The following paragraph presents the fundamental AP-NGD function considered in this paper.

3) AP-NGD Analytical Characterization

For the targeted time-advance $t_0<0$, the AP-NGD TF can be designed with 1st order expression written as:

$$N(s)=1+t_0 s\,. \tag{2}$$

The corresponding magnitude $N(\omega)=|N(j\omega)|$ is given by:

$$N(\omega)=\sqrt{1+t_0^2\omega^2}\,. \tag{3}$$

Hence, the AP-NGD TF GD defined in (1) is expressed as:

$$GD(\omega)=t_0/(1+t_0^2\omega^2)\,. \tag{4}$$

This last expression confirms the AP-NGD behavior of the TF introduced in equation (2) because the GD is always negative whatever ω. The NGD value at very low frequencies (VLFs) $GD(\omega\approx 0)=t_0<0$. This advance is associated to specific angular frequency:

$$\omega_0=2\pi f_0=1/|t_0| \tag{5}$$

At the multiple of this specific angular frequency with positive integer n, we have the magnitude and GD:

$$N(n\cdot\omega_0)=\sqrt{1+n^2} \tag{6}$$

$$GD(n\cdot\omega_0)=t_0/(1+n^2)\,. \tag{7}$$

From these analytical results, the GD and magnitude diagrams shown in Fig. 3(a) and Fig. 3(b) represent the specific characteristics of the AP-NGD analog TF.

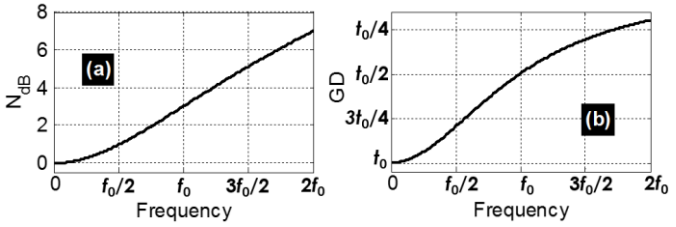

Fig. 3. AP-NGD TF (a) GD and (b) magnitude diagrams.

The GD and magnitude flatness's to preserve the input signal integrity can be assessed. Similar to the design of LP-NGD circuit [35], the integrity of AP-NGD output signal can be guaranteed if the input signal band limitation is lower than $\omega\le 2\omega_0$.

B. AP-NGD First-Order Canonical FIR Design Methodology

The present subsection establishes the original theory of AP-NGD FIR design allowing to generate time advance more than second. The main specifications and characterization of innovative AP-NGD numerical circuit implemented by the canonical FIR are described.

1) Numerical Circuit Architecture Description

The original FIR canonical form is established from the discretization of TF introduced in equation (1). Similar to the LP-NGD numerical circuit design introduced in [35], the AP-NGD FIR design is based on the architecture diagram of Fig. 4 powered by V_{dd}. The architecture has a block of computing core interfaced by Analog Digital Converters (ADC) and Digital Analog Converters (DAC) as input and output interfaces, respectively. The discrete circuit operation is based on internal clock generating the sampling clock supposed with period denoted $\Delta t=T_s=1/f_s$ with f_s is the sampling frequency. Knowing the input signal duration, t_{max}, the numerical architecture must operate with time step following the positive integer index k=0,1,2,…, k_{max}. This maximum is defined by:

$$k_{\max}=\lceil t_{\max}/T_s\rceil \tag{7}$$

knowing that $\lceil\cdot\rceil$ represents the ceiling function.

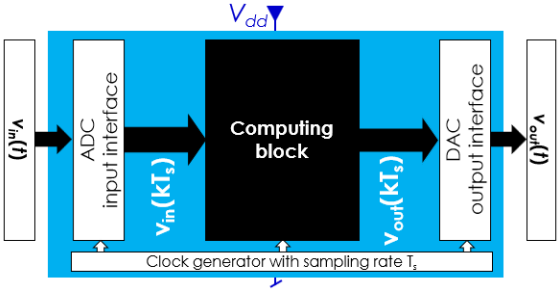

Fig. 4. The considered numerical circuit architecture.

The discrete input and output signals at each instant time $t=kT_s$ are represented by:

$$\begin{cases} v_{in}(k)=v_{in}(kT_s) \\ v_{out}(k)=v_{out}(kT_s) \end{cases}. \tag{8}$$

2) AP-NGD FIR Canonical Form

The original numerical AP-NGD function is elaborated from first-order equation (1). The TF equivalent discrete form is derived from the equivalent differential equation governing input v_{in} and output v_{out}. To realize the time-advance behavior related to the AP-NGD function, the input signal bandwidth should respect condition $\omega_{\max}\le\omega_0$. The analytical combination of equation (2) and $V_{out}(s)=N(s)\cdot V_{in}(s)$ implies the Laplace symbolic equation:

$$V_{out}(s)=V_{in}(s)+t_0 sV_{in}(s)\,. \tag{9}$$

By supposing that the input signal is generated under the initial condition $v_{in}(t=0)=0$. It can be derived with Laplace inverse transform the time-dependent differential equation:

$$v_{out}(t)=v_{in}(t)+t_0\frac{dv_{in}(t)}{dt}\,. \tag{10}$$

The discrete TF is designed by taking into account to initial condition $v_{out}(0)=v_{in}(1)=v_{in}(0)=0$. The AP-NGD function discretization is established from the differential infinitesimal elements:

$$dv_{in}(t)/dt\Rightarrow\delta v_{in}(kT_s)/\delta t\,. \tag{11}$$

By denoting the integer k=0,1,2,…,$k_{\max}$-1, we have the discrete quantities expressed as:

$$\delta v_{in}(kT_s)/\delta t=f_s\left[v_{in}(k+1)-v_{in}(k)\right]. \tag{12}$$

Substituting previous equation (12) into equation (10), the numerical AP-NGD difference equation can be fundamentally formulated by:

$$v_{out}(k+1)=a_1 v_{in}(k+1)+a_0 v_{in}(k) \tag{13}$$

where the FIR coefficient design equations:

$$\begin{cases} a_0 = f_s\, t_0 < 0 \\ a_1 = 1 - f_s\, t_0 \end{cases}. \quad (14)$$

In other words, the AP-NGD FIR can also be designed with coefficient relationship:

$$a_1 = 1 - a_0. \quad (15)$$

C. Characterization and Properties of AP-NGD FIR

The performances of AP-NGD FIR can be quantified based on their characteristics by means of transient tests. The present section describes the basic characteristics and property of the AP-NGD FIR necessary to be respected before the design phase.

1) Transient Characterization from AP-NGD FIR Responses

The signal integrity performance of AP-NGD FIR depends on the transient parameters: time-advance, Δt=t_0, input-output signal gain or attenuation, g, and cross correlation, r. Fig. 5 illustrates the extraction technique of the corresponding parameters.

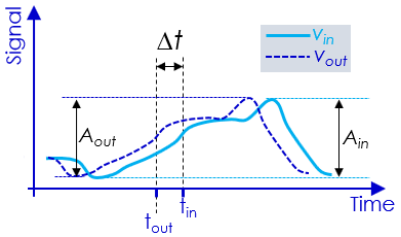

Fig. 5. Illustration of AP-NGD transient characterization.

By choosing a threshold, v_T, the transient time-advance can be expressed as:

$$\begin{cases} \Delta t = t_{out} - t_{in} \\ v_{in}(t_{in}) = v_{out}(t_{out}) = v_T \end{cases} \quad (16)$$

For the case of pulse signal test, we can define this advance as Δt_{rise} or Δt_{fall} depending on the given time interval of input rising or falling fronts. By taking the input and output signal amplitudes A_{in} and A_{out}, the AP-NGD transient gain is given by:

$$g = A_{out} / A_{in}. \quad (17)$$

The input and output relative cross-correlation is expressed as:

$$r(v_{in}, v_{out}) = \frac{\sum_{k=1}^{k_{\max}} \left[v_{in}(k) - \hat{v}_{in}\right]\left[v_{out}(k) - \hat{v}_{out}\right]}{\sqrt{\left(\sum_{k=1}^{k_{\max}} \left[v_{in}(k) - \hat{v}_{in}\right]^2\right)\left(\sum_{k=1}^{k_{\max}} \left[v_{out}(k) - \hat{v}_{out}\right]^2\right)}} \quad (18)$$

where $\hat{v}_{in}$ and $\hat{v}_{out}$ are the input and output averages which are given by the equation, respectively:

$$\hat{v}_{\psi} = \sum_{k=1}^{k_{\max}} v_{\psi}(k) / k_{\max}. \quad (19)$$

with subscript $\psi = \{in, out\}$.

2) Properties of the Developed AP-NGD FIR

The original AP-NGD FIR has some specific properties described as follows:

- The initial value of the discrete variable allowing to realize a reasonable prediction must be:

$$k_0 = \lceil f_s \cdot t_0 \rceil \quad (20)$$

  As explanation, this property corresponds to the first instant time where the output v_{out} gives the correct prediction of input signal value. This property must be satisfied because when $t<|t_0|$, information $v_{out}(t-t_0) \approx v_{in}(t-t_0)$ does not exist with respect to the causality.
- The time-advance effect accuracy can be reached under condition:

$$|t_0| \geq 4 / f_s \Leftrightarrow f_s |t_0| \geq 4. \quad (21)$$

  As explanation, this property corresponds to the accuracy of the predicted output voltage $v_{out}(k \cdot t_s)$. We expect at least an advanced absolute value for times transient samples to guarantee accurate NGD FIR prediction.
- The variations of first order AP-NGD FIR coefficients a_0 and a_1 are mapped versus sampling frequency and time-advance in Fig. 6 in the range of $f_s \in$ [10 mHz,2 Hz] and $t_0 \in$ [-11 s,-1 s]. As results, we have the minimum and maximum of a_0 and a_1 for these ranges of targeted specifications indicated in Table I.

TABLE I
MIN AND MAX OF COEFFICIENTS a_0 AND a_1

Coefficients	a_{0min}	a_{0max}	a_{1min}	a_{1max}
Value	-22	-0.01	1.01	23

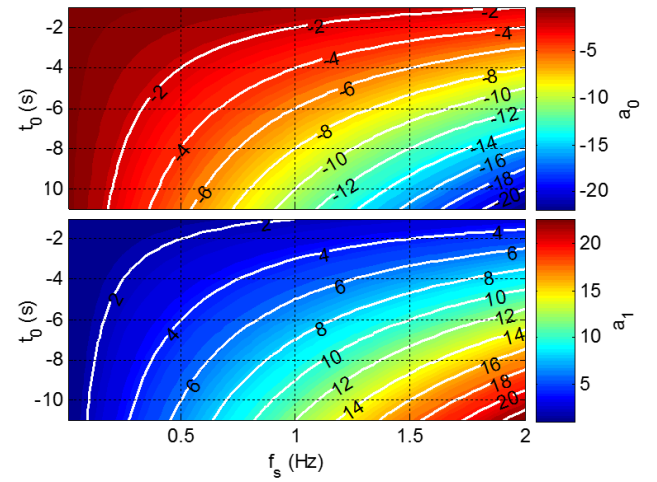

Fig. 6. AP-NGD FIR coefficients (a) a_0 and (b) a_1 versus targeted pair (f_s,t_0).

The following section examines the experimental validation results of the original AP-NGD FIR implemented on STM32® microcontroller unit (MCU) board.

III. Design, Implementation and Test Validation of Original AP-NGD FIR Numerical Circuit

This section is focused on the validity of the original AP-NGD FIR theory. As POC, a numerical circuit is implemented on STM32® MCU test board. The validation study is based on time-domain demonstrations with Gaussian and *sinc* deterministic pulses as input test signals. Then, result of arbitrary waveform, pulse duration and noisy test signal is also discussed. Thus, an AP-NGD potential application for sensor fault diagnosis is described.

A. Description of AP-NGD FIR Implementation

To perform the validation tests, the AP-NGD FIR numerical circuit was implemented on a Nucleo L476RG development board using an STM32L476RG MCU [36]. The 64-pin MCU board is fed by V_{dd}=5 V_{DC} power from USB connector. The microprocessor operates with 12-bit precision ADC for the input- and DAC for the output- analog voltage. The test signal dynamic range is between V_{min}=0 V to V_{max}=3.3 V and quantum

resolution equal to ΔV=800 µV under low sampling frequency f_s=167 mHz. Then, the introduced AP-NGD FIR function was coded in C-language program as indicated by Algorithm I. In this case of study, we target to break the time-advance record by expecting to choose the specification t_0=-10 s. The designed, implemented, and tested AP-NGD IIR coefficients are {a_0=-5/3, a_1=8/3}. The test program was executed by applying analog input voltage applied on pin PA0 converted into digital processed data.

Algorithm I: AP-NGD FIR implemented code.

```
1: float a0 = -1.667; float a1 = 2.667;
2: float vin_1 = 0; float vin_0 = 0; float vout = 0;
3: return float Process(float input)
4: {
5:     //Update internally stored input at t-1
6:    vin_1 = vin_0;
7:     //Update internally stored input at t
8:     vin_0 = input;
9:     //Compute output
10:     vout = a1*vin_1+a0*vin_0;
11:     return vout;
12: }
```

B. Experimental Setup of Original AP-NGD FIR Circuit

Fig. 7(a) represents the experimental setup photograph of original AP-NGD FIR test board. The input and output test signals are transmitted to the oscilloscope through a 1 m-long identical cable. The input signal v_{in} is provided by the signal generator. Then, it attacks the MCU and visualized simultaneously with the output analog voltage from pin PA5 through the DAC. As seen in Fig. 7(b), the MCU is powered by USB port connected to the PC driver.

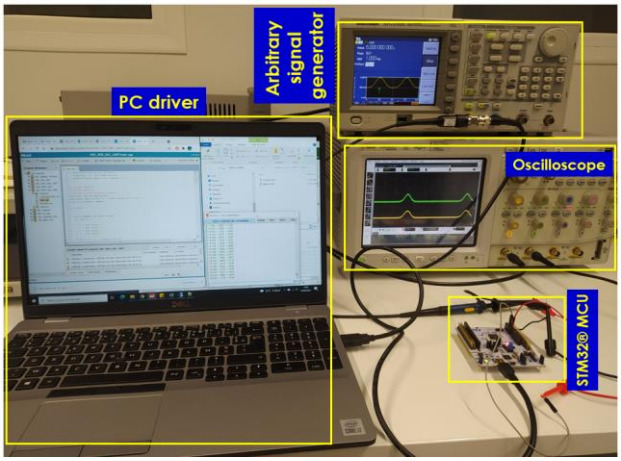

(a)

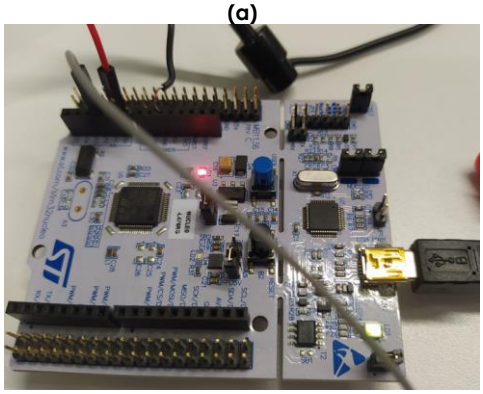

(b)

Fig. 7. Photograph of the (a) AP-NGD FIR experimental setup and (b) the STM32® MCU used test board [36].

During the operation test, the MCU configuration including the input and output signal interactions with the microprocessor is carried out by using the STM32CubeIDE software installed on the PC driver. Thus, the oscilloscope input impedance is configured as R_{in}=1 GΩ. The employed test equipment specifications are addressed in Table II. The tested signal AP-NGD FIR responses are recorded in *csv* format and replotted in MATLAB® environment. Doing this, time-domain test based on deterministic signals presenting possibility to control specifications as bandwidth, magnitude and rise/fall fronts is needed. Accordingly, the AP-NGD FIR transient characterizations with respect to the approaches proposed in paragraph II-B-2 are discussed in the following subsections.

TABLE II
TEST EQUIPMENT SPECIFICATIONS

Description	Reference	Parameter	Value
Arbitrary function generator	Tektronix AFG3102C Dual Channel	Sampling rate	1 GS/s
		Bandwidth	100 MHz
Digital Oscilloscope	Agilent Infiniium MSO8104A	Resolution	12.5 mV
		Sampling rate	4 GSa/s
		Bandwidth	1 GHz
		Channels	4

C. Gaussian Waveform Test Signal-Based AP-NGD FIR Validation

The Gaussian pulse constitutes one of the most relevant characterization test signals of NGD circuit in the time-domain. This subsection is focused on Gaussian waveform pulse voltage with duration [0,t_{max}] and t_{max}=6.7 minutes (min). For the test reproducibility, the input signal analytical expression is given by:

$$v_{in}(t) = V_{\max} \exp\left\{-5\pi^2 f_a^2 (t-\tau)^2 / \left[a_{dB} \ln(10)\right]\right\} \qquad (20)$$

with amplitude, $V_{\max} = v_{in}(\tau)$ =1 V at instant time, τ =3.23 min and a_{dB} is the Gaussian spectrum attenuation at frequency, f_a=1 Hz. Fig. 8(a) displays the time-advance behavior validation of the implemented AP-NGD FIR circuit. The experimented result corresponds to the Gaussian pulse input signal provided by the generator and injected to the MCU.

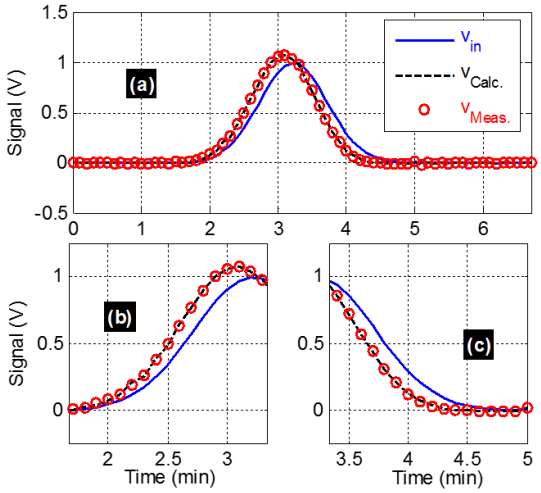

Fig. 8. Calculated and measured AP-NGD FIR Gaussian pulse transient results with (a) wide- and short-duration from (b) [1.6 min, 3.3 min] and (c) [3.3 min, 5 min].

In difference to the analytical one, the input and output test results are recorded from the digital oscilloscope in real-time. A very good agreement between the outputs from MATLAB® calculation, $v_{Calc.}$, (black dashed curve) and measured, $v_{Meas.}$, (red dotted curve) one. To illustrate more obviously the time-advance property, zoom in plots of transient results in [1.6 min, 3.3 min] and [3.3 min, 5 min] are presented in Fig. 8(b) and Fig. 8(c), respectively. As seen in Fig. 8(b) (resp. Fig. 8(c)), the AP-NGD FIR circuit transient response presents outstanding output signal time-advance of leading- (resp. tailing-) edges. By taking threshold voltage V_T=V_{max}/2, Table III quantifies the AP-NGD transient characterization parameters. It is noteworthy that the numerical AP-NGD MCU input and output signal cross correlations are better than 96%.

TABLE III
COMPARISON OF CALCULATED AND MEASURED AP-NGD FIR TRANSIENT CHARACTERISTICS OF GAUSSIAN WAVEFORM INPUT

Parameters	Δt_{rise}	Δt_{fall}	g	r
Calculation	-9.76 s	-9.45 s	1.081	96.6%
Measurement	-9.8 s	-9.38 s	1.083	96.49%

D. AP-NGD FIR Validation with Sinc Waveform Test Signal

In addition to the previous test case, *sinc* waveform pulse voltage was also tested to show the relevant of the designed and implemented AP-NGD FIR circuit by considering duration [0,t_{max}=3.85 min]. In this test case, we would like to demonstrate the AP-NGD FIR circuit flexibility by assuming the targeted time-advance t_0=-2 s different to the previous one. Therefore, the designed, implemented and tested AP-NGD FIR coefficients are {a_0=-2, a_1=3}. In this case, the input signal is analytically determined by:

$$v_{in}(t) = V_{\max} \sin\left[2\pi f_b (t-\tau)\right] / \left[2\pi f_b (t-\tau)\right] \qquad (21)$$

with $V_{\max} = v_{in}(\tau)$ =1 V at instant time, τ =1.433 min and frequency, f_b=1 Hz. Same as the previous case of test, the sinc pulse signal was provided by the generator and injected to the AP-NGD FIR with real-time visualization of input and output simultaneously. As result, Figs. 9 highlight a very good agreement between the calculated and measured test results.

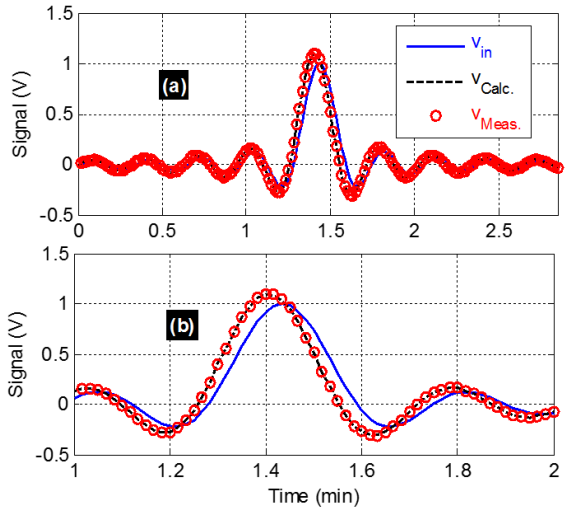

Fig. 9. Calculated and measured AP-NGD FIR transient response of *sinc* waveform pulse with (a) wide- and (b) short-duration representation.

Once again, as seen in the zoom in plot from [1 min,2 min], the -2 seconds time-advance was successfully experimented with *sinc* wave pulse test signal. Moreover, the AP-NGD FIR outputs present the counterintuitive leading- and tailing- edge time advance. Table IV quantifies the AP-NGD transient characterization parameters of *sinc* waveform input. In addition to the analytical input signal test, computational investigation with more industrial context of sensored arbitrary waveform signals plotted in several hours and very long-time duration is examined in the following paragraph.

TABLE IV
COMPARISON OF CALCULATED AND MEASURED AP-NGD FIR TRANSIENT CHARACTERISTICS OF *sinc* WAVEFORM INPUT

Parameters	Δt_{rise}	Δt_{fall}	g	r
Calculation	-1.9 s	-1.9 s	1.098	93.6%
Measurement	-1.8 s	-1.8 s	1.101	93.4%

E. AP-NGD FIR Fast-Pulse Signal Responses

The validity of AP-NGD FIR circuit was validated with two different fast signals presenting milli-second scale pulse duration in real-time by using the same MCU introduced by Figs. 7. Gaussian signal with t_{max}=2 s duration was tested by expecting time-advance t_0=-100 ms. As seen in Fig. 10(a), the calculated and measured signals are in very good agreement. Moreover, sinc with pulse width of about 200 ms and t_{max}=685 ms duration was also tested. As depicted in Fig. 10(b), the advanced effect was once again observed with very good agreement between calculation and measurement. Table V summarizes the measured time-advance, amplification and correlation coefficient. Emphatically, the AP-NGD FIR circuit works very well with less than 1 minute duration faster signals. We underline also that the proposed circuit works very well even for milli- and micro-second duration sensor signals.

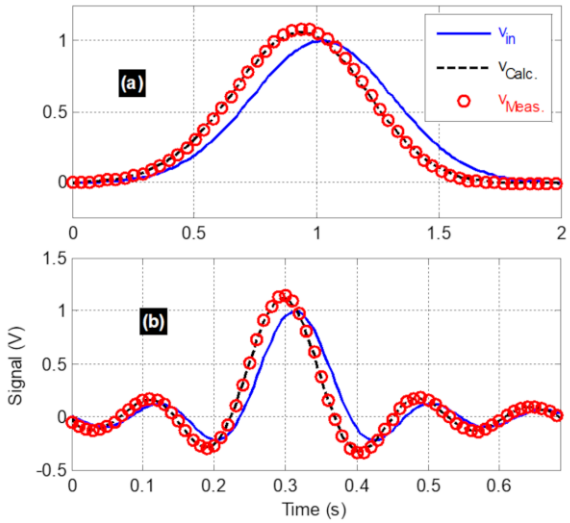

Fig. 10. Calculated and measured AP-NGD predicted results of (a) Gauss(t_{max}=2 s) and (a) sinc(t_{max}=685 ms) fast-signals.

TABLE V
AP-NGD FIR TRANSIENT CHARACTERISTICS OF FAST SIGNALS

Signal	a_0	a_1	Δt_{rise}	Δt_{fall}	g	r
Gauss	-8.336	9.336	84 ms	95 ms	1.06	94.5%
Sinc	-3.963	4.963	15.1 ms	14.9 ms	1.13	92%

F. AP-NGD FIR Responses of Noisy Input

The relevance of AP-NGD FIR circuit with real sensor effect is confirmed by noisy signal tests. To investigate analytically

the AP-NGD FIR circuit versus sensor noise effect, we consider the Gaussian input of Fig. 10(a) with input presenting signal-to-noise (S/N) ratio higher than 40 dB and noise bandwidth $BW_{noise}>50f_0$. The transient responses of input with S/N=60 dB, 50 dB and 40 dB are plotted in Fig. 11(a), 11(b) and 11(c), respectively. Accordingly, the output signal advance is less considerable for S/N<40 dB.

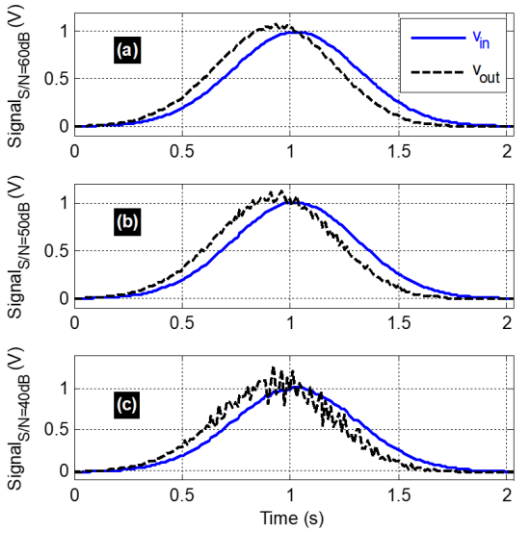

Fig. 11. AP-NGD FIR responses of input signal presenting S/N={(a) 60 dB, (b) 50 dB, (c) 40 dB}.

G. AP-NGD FIR Test Validation of Arbitrary Waveform Sensored Slow Signal

A sensored arbitrary waveform signal was effectively tested with t_0=-10 s time-advance implemented AP-NGD FIR circuit. Fig. 12(a) represents the synoptic diagram of the sensored signal scenario. It includes a potentiometer with time-dependent resistor $R(t)$ with varied from 0 to R_{max}=10 kΩ associated to conditioning circuit comprised of resistors R_1=R_2=2.2 kΩ fed by DC power supply V_f=3.3 V.

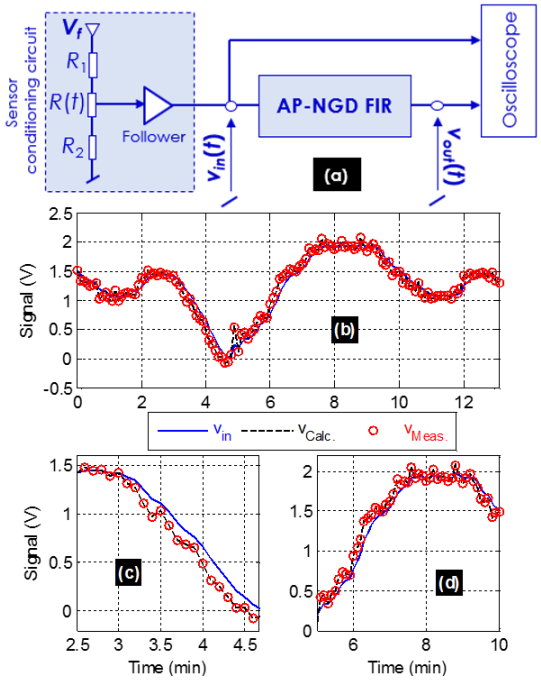

Fig. 12. Sensored signal based AP-NGD (a) experimental setup, and response in time-intervals (b) [0, 13 min], (c) [2.5 min, 4.7 min] and (d) [5 min, 10 min].

In this test case, the experimental setup is constituted by sensor circuit and AP-NGD FIR board interfaced by a follower and terminated by the oscilloscope to visualize in real-time simultaneously voltages v_{in} and v_{out}. To generate the arbitrary waveform test signal, $R(t)$ was randomly and instantaneously varied from minimal to maximal value during, T_{max}=13 min. The long-range calculated and measured output signals are plotted in Fig. 12(b). To highlight the time-advance behavior of the arbitrary signal rise front, the transient result in time-interval [2.5 min, 4.7 min] is zoomed-in Fig. 12(c). The mean time-advance of about Δt_1= -9.1 s is assessed. Furthermore, the plot of Fig. 12(d) shows the time-advance effect on the fall front in the part of test signal in time-interval [5 min, 10 min] is zoomed-in Fig. 12(d). This fascinating test result confirms the feasibility of arbitrary waveform signal anticipation representing typically temporal slow variation. We emphasize that in this test case, the cross correlation between the input-output sensored signal is 91%.

H. Comparison Study of NGD Function

To highlight the originality and effectiveness of the developed AP-NGD test results, comparison study of time-domain approach with respect to the existing work [24-35] on NGD circuit engineering is proposed in this section. Table VI addresses the main objects of comparison based on the NGD circuit characteristics and nature. We can understand from this table that only some of available studies [24,27,29-30-33,35] of the NGD investigation with time-domain experimental tests because it requires challenging efforts. Most of performed NGD circuit engineering are focused on active analog circuit topologies [24-32]. But despite the design simplicity, such analog circuit topologies are not able to operate with more than some seconds in time-advance absolute value. Because of lumped component fabrication technology limitations, the NGD analog topologies are simply limited to the operation from nano- to milli-second time scales.

TABLE VI
COMPARISON OF NGD CIRCUIT CHARACTERISTICS AND NATURE

Reference	Nature	Test	Design	Time scale limit
[24,29-30]	LP-NGD analog active	Yes	Operational amplifier and lumped component	Micro- to milli-seconds
[25]	LP-NGD analog active	No	TF design equation	Nano- to some-seconds
[26]	BP-NGD analog active	No	TF design equation	Nanoseconds
[27,31-32]	LP-NGD analog active	Yes	Transistor and lumped component	Nano- to milli-seconds
[34]	LP-NGD numerical FIR and IIR	No	Design equation	Theoretically illimited
[35]	LP-NGD numerical IIR	Yes	Microcontroller	Milli-seconds to hours
This work	AP-NGD numerical FIR	Yes	Microcontroller	Milli-seconds to hours

Compared to the only available study of NGD numerical circuit engineering [35] achieved with time-domain experimentation, the performed work originality is emphasized with the first exploration of AP-NGD function and the first experimentation of NGD with several seconds time-advance.

IV. Brief Description of NGD Circuit Application for Sensor Fault Diagnosis

An efficient real-time prediction technique is expected to be a relevant solution against the sensor fault diagnosis [1-10]. As typical application, it was proposed that the temporal advance detection with NGD function was exploited to develop analog circuits for medical anticipatory application [24-25]. As reported in [37-39], there are different criteria standards in function of the medical signals under consideration. For example, the blood glucose concentration level which should be predicted with the most significant time advance during the monitoring period. For this case of application, the pulse signal duration can take several hours [37-38]. Then, the systolic and diastolic blood pressure prediction with expected standard threshold is several days pulse duration signals which should be predicted for the remote treatment of patient [39]. The principle of technological NGD solution for sensor fault diagnosis dedicated to real-time diagnosis of industrial control systems is proposed in the present section.

A. Operation Principle of Sensor Fault Detection

To highlight the NGD diagnosis, we can consider an industrial sensor integrating fault detection method in real-time. The operation principle of the sensor NGD diagnosis is illustrated by the synoptic diagram of Fig. 13. In this diagram, we assume that by applying input under the operation process, the sensor is generating time-dependent output parameters $x(t)$.

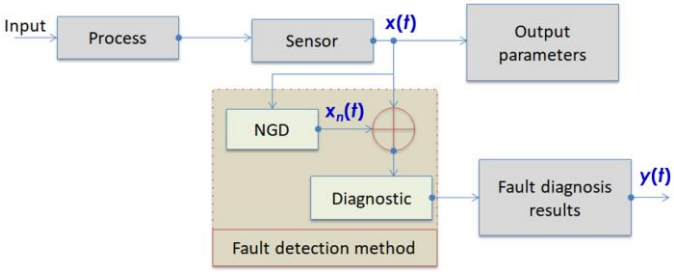

Fig. 13. Synoptic diagram illustrating sensor fault NGD diagnosis.

The sensor fault detection method is performed by three block functions combining x, NGD function with predicted output x_n. The fault diagnosis results are indicated by general output y.

B. Description of Sensor Fault NGD Diagnosis Solution

The real-time fault state of the sensor can be detected in function of its x output level in its operation environment. By injecting the sensor output into the NGD function, advanced signal x_n is generated. Depending on the application cases, this output may not exceed nominal limit for example denoted x_{lim}. Fig. 14(a) presents the real-time plots of arbitrary signals representing the sensor output signals. In this configuration, the considered sensor operates safely if error $x_n(t)<x_{lim}$ as shown in Fig. 14(a). As illustrated by the interaction arrow between Fig. 14(a) and Fig. 14(b), the prediction of sensor fault state can be predicted thanks to the use of NGD function.

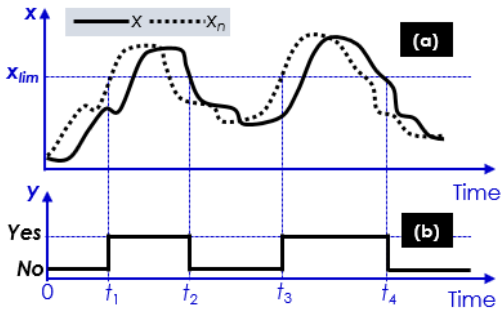

Fig. 14. Illustrative temporal variations of (a) sensor analog output and (b) diagnosis state result.

We can describe the sensor diagnosis results by two binary states as follows:

- In the first case where, the sensor presents fault state, we have y="*YES*". This phase is indicated in interval $t \in \left[t_1, t_2\right] \cup \left[t_3, t_4\right]$ of Fig. 14(b).
- In the other case, the sensor operates safely, the NGD diagnosis is equal to y="*NO*". This state can be seen in intervals $t \in \left[0, t_1\right] \cup \left[t_2, t_3\right] \cup \left[t_4, +\infty\right[$ of Fig. 14(b).

This NGD diagnosis can be operated systematically in real-time during the lifetime of the sensor.

C. NGD Analysis Method to Overcome Sensor Failure Situation

As ongoing research, the developed AP-NGD FIR circuit is expected to overcome the issues of industrial systems victim of sensor failure in real-time. The analysis method for such an application can be introduced as follows:

- Step 1: Based on the time scale (speed and duration) and amplitude of the failure signal signature, an NGD circuit suitable to the targeted application can be designed and implemented.
- Step 2: The NGD circuit is able to predict the failure signal signature in real-time.
- Step 3: Based on the prediction effect, the NGD method enables to pre-detect failure of sensors in real-time.
- Step 4: The pre-detection can be exploited to activate an anticipatory or prevent system in order to avoid the damage effects caused by the failure in the overall industrial system using the default sensor.

V. Conclusion

The NGD concept is one of less familiar functions for electronic engineers. So far most of NGD design research works [24-25,27-33] are focused to LP-NGD ones implemented with analog circuits. Therefore, considerable studies must be developed to familiarize non-specialist engineers to this fascinating AP-NGD numerical functions.

An original engineering of AP-NGD FIR dedicated to non-specialist electronic and industrial engineers is investigated. The present innovative NGD engineering study includes the design, implementation and test methodology. The proposed theory of AP-NGD numerical function is established from elementary circuit represented by a first-order analog TF. The design equation enabling to determine the AP-NGD FIR parameters as the time-advance is established in function of the

implementation plate-form. The transient characterization approach allowing to assess the AP-NGD performance is introduced.

The feasibility of AP-NGD theory is originally validated with STM32® MCU board. A numerical AP-NGD FIR circuit POC is designed and implemented. A record of time-advance equal to -10 seconds ever being experimentally tested is performed. Three test cases of Gaussian, *sinc* and arbitrary waveform signals are presented. As expected, outstanding results showing a very good correlation between the MATLAB® calculations and experimentations are emphasized.

The sensor fault diagnosis constitutes a challenging task for industrial sensor design engineers [1-10]. In this study, an original solution of AP-NGD FIR industrial application for the sensor fault diagnosis is described. The basic principle of the sensor NGD diagnosis and control is introduced by means of illustrative synoptic diagram. The sensor fault NGD diagnosis technique with consideration of AP-NGD time-advance for the error prediction is discussed.

REFERENCES

[1] X. Gong and W. Qiao, "Current-Based Mechanical Fault Detection for Direct-Drive Wind Turbines via Synchronous Sampling and Impulse Detection," *IEEE Trans. Industrial Electronics*, vol. 62, no. 3, pp. 1693-1702, Mar. 2015.

[2] L. Zhang and G. Yang, "Observer-Based Adaptive Decentralized Fault-Tolerant Control of Nonlinear Large-Scale Systems With Sensor and Actuator Faults," *IEEE Trans. Industrial Electronics*, vol. 66, no. 10, pp. 8019-8029, Oct. 2019.

[3] Y. Yao, B. Xie, L. Lei, Y. Li and Q. Yin, "Signal Enhancement Method for Mechanical Fault Diagnosis in Flexible Drive-Train," *IEEE Trans. Industrial Electronics*, vol. 68, no. 3, pp. 2554-2563, Mar. 2021.

[4] C. Kwan and R. Xu, "A note on simultaneous isolation of sensor and actuator faults," *IEEE Trans. Control Systems Technology*, vol. 12, no. 1, pp. 183-192, Jan. 2004.

[5] L. Rajaoarisoa and M. Sayed-Mouchaweh, "Adaptive online fault diagnosis of manufacturing systems based on DEVS formalism," *IFAC-PapersOnLine*, vol. 50, no. 1, July 2017, pp. 6825-6830.

[6] N. Zhou, L. Luo, G. Sheng and X. Jiang, "High Accuracy Insulation Fault Diagnosis Method of Power Equipment Based on Power Maximum Likelihood Estimation," *IEEE Trans. Power Delivery*, vol. 34, no. 4, Aug. 2019, pp. 1291-1299.

[7] P. Segovia, J. Blesa, K. Horvath, L. Rajaoarisoa, F. Nejjari, V. Puig and E. Duviella, "Modeling and fault diagnosis of at inland navigation canals," *Proc. the Institution of Mechanical Engineers, Part I: Journal of Systems and Control Engineering*, vol. 232, no. 6, 2018, pp. 761-771.

[8] P. Segovia, J. Blesa, E. Duviella, L. Rajaoarisoa, F. Nejjari and V. Puig, "Sensor fault diagnosis in inland navigation networks based on a grey-box model," *10th IFAC Symposium on Fault Detection, Supervision and Safety for Technical Processes*, 29-31 Aug. 2018. Warsaw, Poland, vol. 51, no. 24, pp. 742-747, 2018.

[9] D. Alves, J. Blesa, E. Duviella and L. Rajaoarisoa, "Robust Data-driven leak localization in Water Distribution Networks using pressure measurements and topological information," *Sensors journal, MDPI*, vol. 21, no. 7551, Sept. 2021, pp. 1-19.

[10] M. Dzaferagic, N. Marchetti and I. Macaluso, "Fault detection and classification in Industrial IoT in case of missing sensor data," *IEEE Internet of Things Journal*, Early Access, 2021, doi: 10.1109/JIOT.2021.3116785

[11] A. W. Colombo et al., "A 70-Year Industrial Electronics Society Evolution Through Industrial Revolutions: The Rise and Flourishing of Information and Communication Technologies," *IEEE Industrial Electronics Magazine*, vol. 15, no. 1, pp. 115-126, Mar. 2021.

[12] T. Ainsworth, J. Brake, P. Gonzalez, D. Toma and A. F. Browne, "A Comprehensive Survey of Industry 4.0, IIoT and Areas of Implementation," *in Proc. SoutheastCon 2021*, Atlanta, GA, USA, 10-13 Mar. 2021, pp. 1-6.

[13] H. -J. Korber, H. Wattar and G. Scholl, "Modular Wireless Real-Time Sensor/Actuator Network for Factory Automation Applications," *IEEE Trans. Industrial Informatics*, vol. 3, no. 2, pp. 111-119, May 2007.

[14] S. Liu, X. Wang and P. X. Liu, "Impact of Communication Delays on Secondary Frequency Control in an Islanded Microgrid," *IEEE Trans. Industrial Electronics*, vol. 62, no. 4, pp. 2021-2031, Apr. 2015.

[15] A. Maiti, A. A. Kist and A. D. Maxwell, "Real-Time Remote Access Laboratory With Distributed and Modular Design," *IEEE Trans. Industrial Electronics*, vol. 62, no. 6, pp. 3607-3618, June 2015.

[16] P.-Y. Chen, S. Yang and J. A. McCann, "Distributed Real-Time Anomaly Detection in Networked Industrial Sensing Systems," *IEEE Trans. Industrial Electronics*, vol. 62, no. 6, pp. 3832-3842, June 2015.

[17] N. Jalili and E. Esmailzadeh, "Optimum active vehicle suspensions with actuator time delay," *Trans. ASME*, vol. 123, no. 1, Mar. 2001, pp. 54-61.

[18] F. Wilches-Bernal, R. Concepcion, J. C. Neely, D. A. Schoenwald, R. H. Byrne, B. J. Pierre and R. T. Elliott, "Effect of Time Delay Asymmetries in Power System Damping Control," *in Proc. 2017 IEEE Power & Energy Society General Meeting*, Chicago, IL, USA, 16-20 July 2017, pp. 1-5.

[19] Z. S. Veličković and V. D. Pavlović, "Complex analytic signals applied on time delay estimation," *Physics, Chemistry and Technology*, vol. 6, no. 1, pp. 11-28, 2008.

[20] H. Zhang, Y. Shi, J. Wang and H. Chen, "A New Delay-Compensation Scheme for Networked Control Systems in Controller Area Networks," *IEEE Trans. Industrial Electronics*, vol. 65, no. 9, pp. 7239-7247, Sept. 2018.

[21] B. Ravelo, S. Lalléchère, A. Thakur, A. Saini and P. Thakur, "Theory and circuit modelling of baseband and modulated signal delay compensations with low- and band-pass NGD effects," *Int. J. Electron. Commun.*, vol. 70, no. 9, Sept. 2016, pp. 1122-1127.

[22] X. Deng, P. Jiang, X. Peng and C. Mi, "An Intelligent Outlier Detection Method With One Class Support Tucker Machine and Genetic Algorithm Toward Big Sensor Data in Internet of Things," *IEEE Trans. Industrial Electronics*, vol. 66, no. 6, pp. 4672-4683, June 2019.

[23] L. Clifton, D. A. Clifton, M. A. F. Pimentel, P.J. Watkinson and L. Tarassenko, "Predictive Monitoring of Mobile Patients by Combining Clinical Observations With Data From Wearable Sensors," *IEEE J. Biomed. Health Inform.*, vol. 18, no. 3, May 2014, pp. 722-730.

[24] C. Hymel, R. A. Stubbers and M. E. Brandt, "Temporally Advanced Signal Detection: A Review of the Technology and Potential Applications," *IEEE Circuits and Systems Magazine*, vol. 11, no. 3, pp. 10-25, Thirdquarter 2011.

[25] H. U. Voss, "Signal prediction by anticipatory relaxation dynamics," *Phys. Rev. E*, vol. 93, no. 3, (030201R), pp. 1-5, 2016.

[26] S.-S. Myoung, B.-S. Kwon, Y.-H. Kim and J.-G. Yook, "Effect of Group Delay in RF BPF on Impulse Radio Systems," *IEICE Trans. Communications*, vol. 90, no. 12, Dec. 2007, pp. 3514-3522.

[27] B. Ravelo, "Similitude between the NGD function and filter gain behaviours," *Int. J. Circ. Theor. Appl.*, vol. 42, no. 10, Oct. 2014, pp. 1016-1032.

[28] B. Ravelo, "First-order low-pass negative group delay passive topology," *Electronics Letters*, vol. 52, no. 2, Jan. 2016, pp. 124–126.

[29] M. W. Mitchell and R.Y. Chiao, "Negative Group-delay and 'Fronts' in a Causal Systems: An Experiment with Very Low Frequency Bandpass Amplifiers," *Phys. Lett. A*, vol. 230, no. 3-4, Jun. 1997, pp. 133-138.

[30] T. Nakanishi, K. Sugiyama and M. Kitano, "Demonstration of Negative Group-delays in a Simple Electronic Circuit," *Am. J. Phys.*, vol. 70, no. 11, 2002, pp. 1117-1121.

[31] B. Ravelo, "Demonstration of negative signal delay with short-duration transient pulse," *Eur. Phys. J. Appl. Phys.* (*EPJAP*), vol. 55, no. 10103, 2011, pp. 1-8.

[32] B. Ravelo, "Methodology of elementary negative group delay active topologies identification", *IET Circuits Devices Syst.* (*CDS*), Vol. 7, No. 3, May 2013, pp. 105-113.

[33] B. Ravelo, "Theory on negative time delay looped system," *IET Circuits, Devices & Systems*, vol. 12, no. 2, Mar. 2018, pp. 175–181.

[34] B. Ravelo, "Elementary NGD IIR/FIR Systems," *Int. J. Signal Processing Systems* (*IJSPS*), vol. 2, no. 2, Dec. 2014, pp. 132-138.

[35] B. Ravelo, M. Guerin, W. Rahajandraibe, V. Gies, L. Rajaoarisoa and S. Lalléchère, "Low-Pass NGD Numerical Function and STM32 MCU Emulation Test," *IEEE Trans. Industrial Electronics*, vol. 39, no. 8, Aug. 2022, pp. 8346-8355.

[36] ST, STM32L476xx, Datasheet-Production Data, pp. 1-270, June 2019.

[37] J. Martinsson, A. Schliep, B. Eliasson, and O. Mogren, “Blood Glucose Prediction with Variance Estimation Using Recurrent Neural Networks,” J. Healthc. Inform. Res., vol. 4, 2020, pp. 1–18.
[38] M. Munoz-Organero, “Deep Physiological Model for Blood Glucose Prediction in T1DM Patients,” Sensors (Basel), vol. 20, no. 3896, Jul. 2020, pp. 1-17.
[39] A. G. Logan, W. J. McIsaac, A. Tisler, M. J. Irvine, A. Saunders, A. Dunai, C. A. Rizo, D. S. Feig, M. Hamill, M. Trudel, and J. A. Cafazzo, “Mobile Phone–Based Remote Patient Monitoring System for Management of Hypertension in Diabetic Patients,” American Journal of Hypertension, Vol. 20, no. 9, Sept. 2007, pp. 942–948.

Prof. Dr. Blaise RAVELO (M’09) is currently University Full Professor at NUIST, Nanjing, China. His research interest is on Multiphysics and electronics engineering. He is a pioneer of the negative group delay (NGD) theory, engineering, development, and application. He is the world most active researcher on NGD topic according to Scopus. This extraordinary NGD concept is potentially useful for anticipating and prediction all kind of information. He was research director of 11 PhD students (10 defended), postdocs, research engineers and Master internships. With US, Chinese, Indian, European and African partners, he is actively involved and contributes on several international research projects. He is member of IET Electronics Letters editorial board as circuit & system subject editor. He is member of scientific technical committee of Advanced Electromagnetic Symposium (AES) and IMOC2021. He is ranked in Top 2% world’s scientists based on years (2020-2021) by Stanford University, US (https://elsevier.digitalcommonsdata.com/datasets/btchxktzyw/3). He has Google scholar h-index(2022)=26 and i10-index(2022)=83. He is member of research groups: IEEE, URSI, GDR Ondes, Radio Society and (co-) authors of more than 370 scientific research papers in new technologies published in int. conf. and journals. He is lecturer on circuit & system theory, STEM (science, technology, engineering and maths) and applied physics. Dr. Ravelo is regularly invited to review papers submitted for publication to international journals (IEEE TRANSACTIONS ON MICROWAVE THEORY AND TECHNIQUES, IEEE TRANSACTIONS ON CIRCUITS AND SYSTEMS, IEEE TRANSACTIONS ON ELECTROMAGNETIC COMPATIBILITY, IEEE TRANSACTIONS ON INDUSTRIAL ELECTRONICS, IEEE ACCESS, IET CDS, IET MAP …) and books (Wiley, Intech Science…).

Dr. Mathieu GUERIN obtained an engineering degree in Microelectronics and Telecommunications from Polytech Marseille in 2010 and at the same time a Research Master in Integrated Circuits Design from the University of Aix-Marseille. He obtained his PhD degree from the same institution in 2013. He worked as technical leader of the analog and radio-frequency design team of IDEMIA-StarChip for five years and designed chips embedded in SIM cards and contactless bank cards with biometric recognition. He joined Aix-Marseille University as an Assistant Professor in 2020 and joined the CCSI team of the IM2NP laboratory. His research focuses mainly on the design and synthesis of circuits in digital electronics. He is also working on methods of modeling and characterizing circuits in analog electronics.

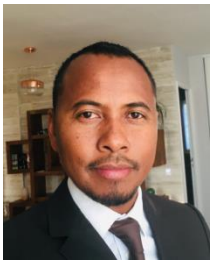

Prof. Dr. Wenceslas RAHAJANDRAIBE is currently full professor at the University of Aix-Marseille. He received the B. Sc. degree in electrical engineering from Nice Sophia-Antipolis University, France, in 1996 and the M. Sc. (with distinction) in electrical engineering from the University of Montpellier, Science department, France, in 1998. Since 1998, he joined the microelectronics department of Informatics, Robotics and Microelectronics Laboratory of Montpellier (LIRMM) and received the Ph. D. on Microelectronics form the University of Montpellier. Since 2003, he joined the microelectronic department of Materials, Microelectronics and Nanoscience Laboratory of Provence (IM2NP) in Marseille, France where he was an Associate Professor. Since 2014, he is Professor at Aix Marseille University where he heads the Integrated Circuit Design group of the IM2NP laboratory. He is regularly involved to participate and to lead national and international research projects (ANR, H2020, FP7 KIC-InnoEnergy…). He directed and co-supervised 18 PhD and 15 Master students. His research interests involve AMS and RF circuit design from transistor to architectural level. His present research activity is focused on ultralow power circuit design for smart sensor interface and embedded electronic in bioelectronic and e-health applications, wireless systems, design technique and architecture for multi-standard transceiver. He is author or co-author of 11 patents and more than 150 papers published in refereed journals and conferences. He is an expert for the ANR, the French Agency for Research. He has served on program committees of IEEE NEWCAS and ICECS. He has been and is a reviewer of contributions submitted to several IEEE conferences and journals such as ISCAS, NEWCAS, MWSCAS, ESSCIRC, ESSDERC, RFIC, IEEE Transactions on Circuits and Systems I and II, IET Electronics Letters.

Dr. Lala RAJAOARISOA is currently an Assistant Professor at the Institut Mines-Télécom Lille Douai. He received his M.Sc. degree and PhD in Automatic and Computer Sciences, both at the University of Aix-Marseille, France in 2005 and 2009. His research interests are the development of data-driven tools and methods for the observation and control of large-scale distributed systems. Develop predictive models and controllers to assess system behavior and optimize its performance. This development includes the analysis of intrinsic properties such as stability, observability, identifiability and controllability. He is involved in research activities dedicated to the optimization of energy efficiency of building systems and the control and management of hydraulic systems with more than 80papers published in refereed journals and conferences. He regularly participates and contributes on several international projects (ANR, FUI, and INTERREG) and was the supervisor of more than of 15 PhD students, postdocs, research engineers and Master internships.